

See discussions, stats, and author profiles for this publication at: <https://www.researchgate.net/publication/257813518>

C60 reduces the bioavailability of mercury in aqueous solutions

Article in *Chemosphere* · October 2013

DOI: 10.1016/j.chemosphere.2013.09.027 · Source: PubMed

CITATIONS

5

READS

71

9 authors, including:



F. Menn

Thermo Fisher Scientific

31 PUBLICATIONS **897** CITATIONS

SEE PROFILE



Tingting Xu

University of Tennessee

20 PUBLICATIONS **262** CITATIONS

SEE PROFILE



Steven Ripp

University of Tennessee

133 PUBLICATIONS **2,275** CITATIONS

SEE PROFILE



Alice Layton

University of Tennessee

168 PUBLICATIONS **3,741** CITATIONS

SEE PROFILE



Contents lists available at ScienceDirect

Chemosphere

journal homepage: www.elsevier.com/locate/chemosphere

C60 reduces the bioavailability of mercury in aqueous solutions



Wen-Juan Shi^a, Fu-Min Menn^{b,c}, Tingting Xu^b, Zibo T. Zhuang^d, Clara Beasley^b, Steven Ripp^b, Jie Zhuang^{b,e,*}, Alice C. Layton^b, Gary S. Saylor^{b,c}

^a Key Laboratory of Northwestern Water Resources and Ecological Environment, Xi'an University of Technology, Xi'an 710048, China

^b Center for Environmental Biotechnology, The University of Tennessee, Knoxville, TN 37996, United States

^c The University of Tennessee/Oak Ridge National Laboratory Joint Institute for Biological Sciences, Oak Ridge, TN 37830, United States

^d Department of Bioengineering, Rice University, Houston, TX 77005, United States

^e Department of Biosystems Engineering and Soil Science, Institute for a Secure and Sustainable Environment, The University of Tennessee, Knoxville, TN 37996, United States

HIGHLIGHTS

- 30% of Hg²⁺ became biologically unavailable when C60 is 1% of the mass of Hg²⁺.
- Increase in C60 dosage reduces mercury bioavailability.
- Reaction time length is more important than C60 dosage.
- Lowering solution pH from 7.2 to 5.8 decreases mercury bioavailability.
- The pH effect is more significant at lower C60 dosages.

ARTICLE INFO

Article history:

Received 7 December 2012

Received in revised form 5 September 2013

Accepted 16 September 2013

Available online 11 October 2013

Keywords:

Nanocarbon

C60

Mercury

pH

Water treatment

Bioreporter

ABSTRACT

The effects of C60 on mercury bioavailability and sorption were investigated at different C60 dosages, reaction times, and pH ranges using the *merR::luxCDABE* bioluminescent bioreporter *Escherichia coli* ARL1. The results demonstrated that the bioavailability of mercury (Hg²⁺) decreased with increasing C60 dosage. Approximately 30% of aqueous mercury became biologically unavailable 2 h after interaction with C60 at a mass ratio of C60 to mercury as low as 0.01. However, this reduction in bioavailability plateaued at a mass ratio of C60 to mercury of 10 with a further increase in C60 concentrations resulting in only a 20% additional decrease in bioavailability. If this reduction in bioluminescence output is attributable to mercury sorption on C60, then each one log-order increase in C60 concentration resulted in a 0.86 log-order decrease in the mercury partitioning coefficient (K_d). This relationship implies the presence of high mercury-affinitive sites on C60. The length of reaction time was found to play a more important role than C60 dosage in reducing Hg²⁺ bioavailability, suggesting an overall slow kinetics of the C60–Hg interactions. In addition, lowering the pH from 7.2 to 5.8 decreased mercury bioavailability due likely to the increase in mercury's association with C60. These results suggest that C60 may be useful in capturing soluble mercury and thus reducing mercury biotoxicity.

Published by Elsevier Ltd.

1. Introduction

Maintaining a sufficient supply of clean water for drinking is critical for society, particularly in geographic locations with rapid population growth and urbanization (Reiter et al., 2004). However, contamination of water supply sources continues to be problematic, with heavy metals being of particular concern. Mercury, for example, is highly toxic towards biological systems and, once absorbed by microbiota, becomes bioaccumulated in the food

chain with consequent toxic impacts to higher order animal and human health. Due to mercury's elevated toxicity, stringent regulatory controls have been imposed on mercury concentrations in the environment. For instance, mercury is a priority pollutant that the U.S. Environmental Protection Agency has set a maximum contaminant level of 2 µg L⁻¹ in drinking water (USEPA, 2009).

To protect drinking water, inexpensive and efficient methods for monitoring and removing mercury from natural water and soil runoff are of great interest. Conventional technologies, such as membrane filtration, ion exchange, solvent extraction, and biological degradation, are reasonably efficient for mercury removal (Jones and Slotton, 1996; Nanseu-Njiki et al., 2009; USEPA, 1997), but are relatively costly and time-consuming. Consequently, the search for new and advanced technologies for mercury removal continues. Nanotechnology, using materials and structures with

* Corresponding author. Address: Department of Biosystems Engineering and Soil Science, Center for Environmental Biotechnology, Institute for a Secure and Sustainable Environment, The University of Tennessee, Knoxville, TN 37996-4134, United States. Tel.: +1 (865) 974 9467; fax: +1 (865) 974 4514.

E-mail address: jzhuang@utk.edu (J. Zhuang).

nanoscale dimensions of 1–100 nm, is a promising technology widely studied for water treatment (Colvin, 2003; Masciangelo and Zhang, 2003; Savage and Diallo, 2005). For example, the suitability of nanocarbon and metal oxides in removing different types of water contaminants has been well investigated in the last decade (Meyyappan and Srivastava, 2000). Previous studies mainly focused on nanocarbon tubes or modified traditional sorbents (e.g., active carbon) (Cooper et al., 2010; Tawabini et al., 2010) and indicate that the sorption capacity of nanomaterials for metals primarily depends on their nanosize and surface area.

Theoretically, C60 fullerenes should have an adsorption capacity similar to carbon nanotubes due to their high hydrophobic surface area and large inner volume of spherical structures. Pyrzynska (2007) reported that C60 could extract low polar metal complexes from aqueous solution through π -electron interactions between them, and that maximum chelate adsorption was achieved within a pH range of 0.5–5.0. C60 was also found to exhibit better sorption properties for metal than conventional reversed-phase sorbent materials such as silica-bonded C18. Lesniewska et al. (2005) reported that the neutral chelates of lead, cadmium, and palladium formed with ammonium pyrrolidinedithiocarbamate or diethyldithiocarbamate could be sorbed onto a microcolumn packed with C60. Yoon et al. (2008) found that calcium and strontium could be strongly bound to C60 through charge transfer mechanisms. This charge redistribution, in turn, gives rise to electric fields surrounding the coated C60. Recent studies have suggested that lithium adsorption preferably occurs on C60 in a carbon hybrid material system consisting of single-wall carbon nanotubes (SWCNTs) and C60 due to larger adsorption energy on C60 than on pure SWCNTs (Koh et al., 2011). All of these studies provide insights into the potential of C60 for mercury removal. However, the interaction between mercury and C60 has yet to be carefully investigated, particularly with respect to its effect on mercury bioavailability. The objective of this study was to examine the effects of C60 on the bioavailability and adsorption of mercury under various reaction conditions, including C60 dosage, reaction time, and pH, to better elucidate its potential role in mercury remediation.

2. Materials and methods

2.1. C60 and mercury preparations

C60 powder was maintained dry in a glass bottle at room temperature (22 ± 1 °C) and then dissolved in toluene to create a 2000 mg L⁻¹ C60 suspension (Miyako et al., 2008). This C60 stock solution was further diluted with toluene to prepare a range of C60 experimental dosages from 0.01 to 500 μ g (equivalent to mass ratios of C60 to Hg²⁺ from 0.014 to 675). C60 suspensions were then transferred individually into 100-mL glass bottles and dried in a fume hood at room temperature to volatilize the toluene.

Mercury, in the form of mercury (II) chloride (HgCl₂), was maintained at a stock concentration of 1000 μ g L⁻¹, kept at 4 °C, and filtered through a 0.22 μ m nylon membrane prior to each use. The various experimental dilutions described in Section 3 were performed by diluting the HgCl₂ stock solution in sterile deionized water. For pH experiments, the pH of the mercury solutions was adjusted using diluted 0.05 M HCl or 0.05 M NaOH. Mercury solutions were then combined with the dried C60 and vortexed for 1 min to resuspend the C60.

2.2. Bioluminescent bioavailability assay for mercury

Bioavailable mercury was measured as a function of the bioluminescent emission intensity of the *merR::luxCDABE*-based bioreporter *E. coli* ARL1 using a BioTek Synergy multi-mode micro-

plate reader (Winooski, VT, USA). *E. coli* ARL1 harbors a chromosomally inserted \sim 500 bp region of the *mer* operon consisting of the *merR* gene and the promoter/operator region of the *mer* operon fused to the *luxCDABE* gene cassette of *Photobacterium luminescens* (Dahl et al., 2011). Its detection limit for bioavailable Hg (II) is approximately 2 μ g L⁻¹ and it effectively differentiates between Hg²⁺ and Hg-EDTA complex (Dahl et al., 2011). Bioluminescent assays were performed by growing the ARL1 bioreporter from -80 °C freezer stock in 25 mL Luria–Bertani (LB) broth supplemented with kanamycin at 50 mg L⁻¹ (Kn₅₀) at 30 °C with shaking (200 rpm) to an optical density at 600 nm (OD₆₀₀) of 0.7. The culture was then diluted 1:10 in fresh LB broth + Kn₅₀ and incubated with shaking (200 rpm) at 30 °C to an OD₆₀₀ of 0.30 ($\sim 1 \times 10^8$ cfu mL⁻¹, exponential growth phase). Aliquots of 900 μ l of the culture were then transferred to black 24-well microtiter plate wells (Corning, NY, USA) containing 100 μ l of the HgCl₂/C60 dilutions as explained above. At least three replicates of each 24-well plate were performed and a minimum of three replicates for each dilution were included in each plate. Plates were sealed with a transparent membrane (Breathe-Easy, Sigma–Aldrich, St. Louis, MO, USA) and placed in the BioTek Synergy plate reader for bioluminescence detection at 28 °C. Bioluminescence in counts per second (cps) was recorded with a 1 s integration time every 5 min for 2 h. Each plate contained triplicate controls consisting of *E. coli* ARL1 + HgCl₂ at 1 μ g mL⁻¹, *E. coli* ARL1 alone, *E. coli* ARL1 + 100 μ L toluene, and *E. coli* ARL1 + 500 μ g C60. An additional constitutively bioluminescent bioreporter, *E. coli* 652T7, consisting of a T7 promoter fusion to the *P. luminescens luxCDABE* gene cassette, was included in triplicate in each plate as a control to establish mercury or C60 toxicity (i.e., a loss of bioluminescent light from this bioreporter indicated mercury or C60 concentrations toxic to *E. coli*).

2.3. Experiments establishing C60 exposure time effects

For experiments demonstrating the effect of exposure time of C60 towards mercury bioavailability, mixtures of mercury at 0.74 μ g mL⁻¹ in deionized water were combined with C60 at dosages of 0.01, 0.05, 0.1, 0.5, or 1.0 μ g and incubated at room temperature with shaking (200 rpm) for either 30 min or 120 min, after which aliquots were removed and transferred to 24-well microtiter plates for the determination of bioavailability as described above.

2.4. Data analysis

The amount of mercury adsorbed on C60 was determined by calculating the difference between the initial (C_i) and equilibrium concentrations (C_m). The mercury removal (%) from the solution was calculated as:

$$R = \frac{C_i - C_m}{C_i} \times 100 \quad (1)$$

The metal affinity, indicated by the partitioning coefficient K_d (μ g μ g⁻¹), was calculated as:

$$K_d = \frac{C_i - C_m}{M_d} \times V \quad (2)$$

where V is the solution volume (mL), and M_d is the mass of C60 (μ g).

All tests were performed in at least triplicate and results expressed as the mean \pm standard deviation. Significance was established using an analysis of variance (ANOVA) at $p < 0.05$.

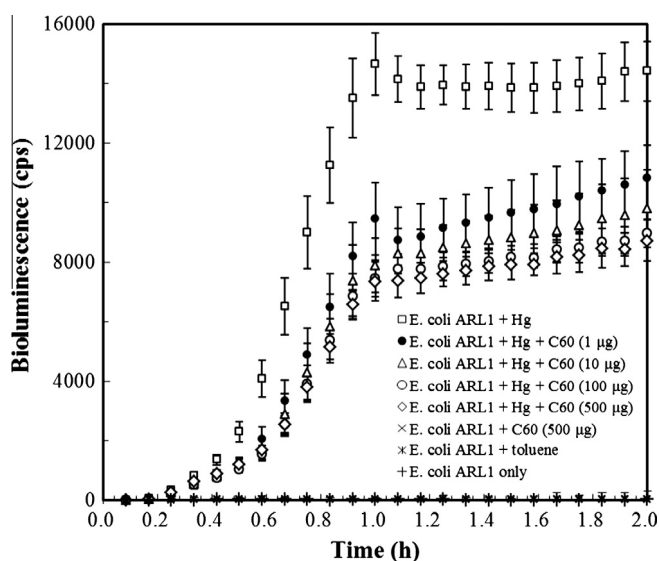


Fig. 1. Bioluminescence emission profile of the *E. coli* ARL1 bioreporter during a 2 h exposure to C60 at dosages ranging from 1 to 500 μg in the presence of a constant $0.74 \mu\text{g mL}^{-1}$ concentration of Hg^{2+} . cps: bioluminescent counts/s.

3. Results and discussion

3.1. Effect of C60 dosage

The effect of C60 on mercury bioavailability was first investigated using dosages of C60 between 1 and 500 μg (corresponding to mass ratios of C60 to Hg^{2+} from 1.35 to 675) under a constant Hg^{2+} exposure concentration of $0.74 \mu\text{g mL}^{-1}$. The results demonstrated that mercury bioavailability, as measured by the bioluminescent bioreporter *E. coli* ARL1, significantly decreased in the presence of C60 and was dose dependent across the 1, 10, 100, and 500 μg C60 dosages tested (Fig. 1). No significant bioluminescence was detected among the controls (*E. coli* ARL1 alone and *E. coli* ARL1 + C60 at 500 μg) nor did *E. coli* ARL1 respond to residual levels of toluene potentially remaining after the C60 preparation. Bioluminescence from the constitutive control bioreporter *E. coli* 652T7 was not significantly affected by C60 or mercury within the experimental concentrations applied, thus demonstrating that C60 and mercury were not themselves toxic towards *E. coli* under our experimental conditions (data not shown).

The *E. coli* ARL1 bioreporter bioluminescence emission profiles were used to indicate Hg^{2+} bioavailability and demonstrated that

Hg^{2+} bioavailability decreased with increasing C60 concentrations (Fig. 2a). The addition of a very small amount of C60 (e.g., 1% of Hg^{2+} mass) reduced Hg^{2+} bioavailability by 30%. However, a further five log-order increase in C60 concentration resulted only in an additional 20% decrease in bioavailability. If the decrease in bioluminescence from *E. coli* ARL1 is attributed to Hg^{2+} adsorption on C60, the partitioning coefficients (K_d) of Hg^{2+} on C60 decreased with increasing C60 dosage (Fig. 2b). The fitted equation indicated that each one log-order increase in C60 concentration resulted in a decrease in the K_d value by an order of 0.86. This moderate inconsistency implies the presence of sorption sites having high affinity for Hg^{2+} . Our calculations indicate that these high-affinity sites may account for approximately 14% of the total sorption sites, with the majority of sites being relatively uniform in affinity for Hg^{2+} . This variability in affinity, however, requires further study through chemical characterization.

3.2. Effect of C60 exposure time on mercury bioavailability

Fig. 3 shows the reduction of bioavailable mercury starting at a concentration of $0.74 \mu\text{g mL}^{-1}$ after exposure to C60 for 30 min versus 120 min at five low C60 dosages (0.01, 0.05, 0.1, 0.5, and 1 μg). These dosages are equivalent to the mass ratios of C60 to Hg^{2+} of 0.014, 0.068, 0.135, 0.675, and 1.354, respectively. The longer exposure time of 120 min reduced mercury bioavailability significantly compared to the 30 min exposure time. The 30 min exposure resulted in less than 5% of the mercury becoming unavailable to the *E. coli* ARL1 bioreporter bacteria, whereas the 120 min exposure resulted in 30–40% of the mercury to becoming unavailable at the experimental dosages. This time dependent reduction in bioavailability is likely due to sorption of Hg^{2+} by C60 since *E. coli* ARL1 responds only to ionic mercury (Hg^{2+}). Once associated with C60, Hg^{2+} is unable to be taken up by *E. coli* ARL1, thus resulting in the reduced bioluminescent response.

3.3. Effect of pH on mercury bioavailability

Fig. 4 shows the effect of pH on the bioluminescence emission profile of *E. coli* ARL1 during interaction with Hg^{2+} at a starting concentration of $0.74 \mu\text{g mL}^{-1}$. Lowering the pH from 7.2 to 5.8 reduced bioluminescence emission over a wide range of mass ratios of C60 to Hg^{2+} (0.01–1.35). This reduction in bioluminescence could be attributed to a decrease in Hg^{2+} uptake by strain ARL1 due to pH-induced alteration of bacterial physiology and/or Hg^{2+} sorption on C60. Previous studies have shown that acidification increases intracellular accumulation of Hg^{2+} and enhances

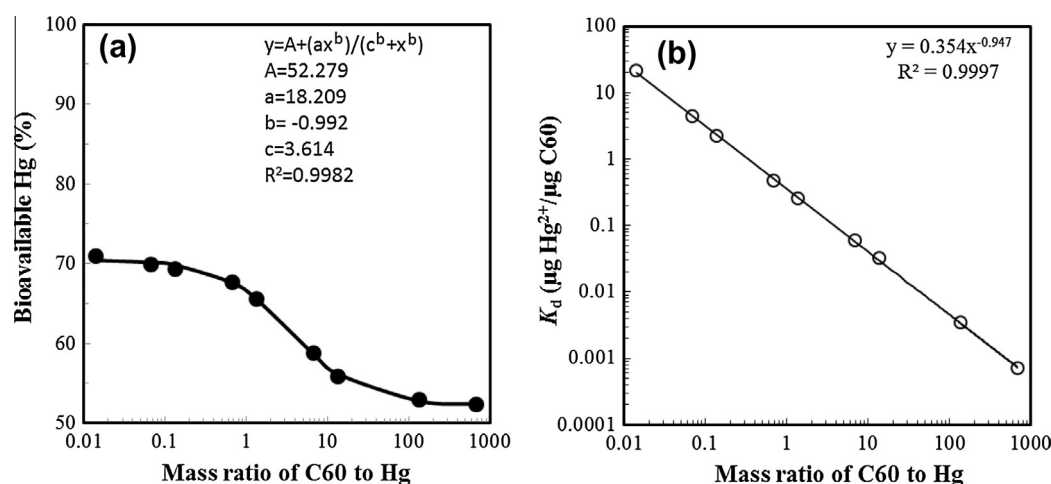


Fig. 2. Effect of C60 on (a) mercury bioavailability and (b) mercury partition coefficient (K_d) after a 2 h exposure at a constant $0.74 \mu\text{g mL}^{-1}$ concentration of Hg^{2+} .

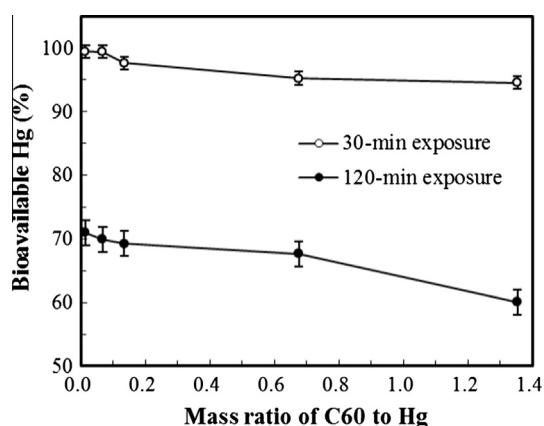


Fig. 3. Effect of exposure time on mercury bioavailability at low mass ratios of C60 to Hg at a constant $0.74 \mu\text{g mL}^{-1}$ concentration of Hg^{2+} .

light emission (Golding et al., 2002; 2008; Kelly et al., 2003). Therefore, the opposite pH effect observed in this study was dominantly caused by enhanced association of Hg^{2+} on C60 at lower pH. As demonstrated by the differences in bioluminescence emission intensity, the pH effect was reduced as C60 dosage increased. This is in accordance with Schindler et al. (1980) who showed that mercury ions bind to organic matter more strongly as solution pH decreases. Tawabini et al. (2010) observed a negligible effect of solution pH on mercury sorption by multiwalled carbon nanotubes (MWCNTs) between pH 5 and 7 at high mass ratios of carbon to mercury (1000–2000:1). However, they reported that mercury removal increased from 73% at pH 4 to 93% at pH 5 and decreased from 95% at pH 8 to 81% at pH 9. They attributed the varying effects at different ranges of pH values to the changes in the surface

charge of MWCNTs and the composition of the aqueous mercury species. Our results suggest that the concentration of carbon nanoparticles is also a factor that influences the pH effect. For example, the pH effect was significantly smaller at the C60:Hg mass ratio of 1.35 than at 0.01 (Fig. 4d versus a). This trend corresponds with the minimal pH effect observed by Tawabini et al. (2010) at high MWCNT dosages (e.g., MWCNT:Hg mass ratios of 1000–2000) in the same range of pH values (i.e., 5–7). Our results indicate that a pH rendered change in surface charge exerts limited effects on mercury association with C60. One of the main mechanisms involved is that of acidification decreasing the concentrations of negative mercury species (e.g., $\text{Hg}(\text{OH})_3^-$ and $\text{Hg}(\text{OH})_4^{2-}$) while increasing the concentration of Hg^{2+} . The latter positively species exhibits stronger adsorption on negatively charged C60 than the former two negatively charged species. As a result, mercury is more strongly bound to C60 at lower pH, leading to decreased bioavailability of mercury to the bioreporter and, thus, lower bioluminescence emission. However, mercury that is associated with environmental media (e.g., colloids) can become bioavailable under certain pH conditions. Such pH-mediated bioavailability would be expected to lead to mercury accumulation in higher organisms (e.g., fish) in surface water with bulk mercury contamination (Jones and Slotton, 1996). Nonetheless, the complicated relationships between solution pH, mercury species, sorption, and bioavailability require further study.

4. Conclusions

Based on the bioavailability profiles of the *E. coli* ARL1 bioluminescent bioreporter, it was demonstrated that C60 is efficient in reducing the bioavailability of Hg^{2+} through association primarily mediated by sorption. The sorption efficiency varies with C60 dosage, reaction time, and pH. Specific findings of this study are:

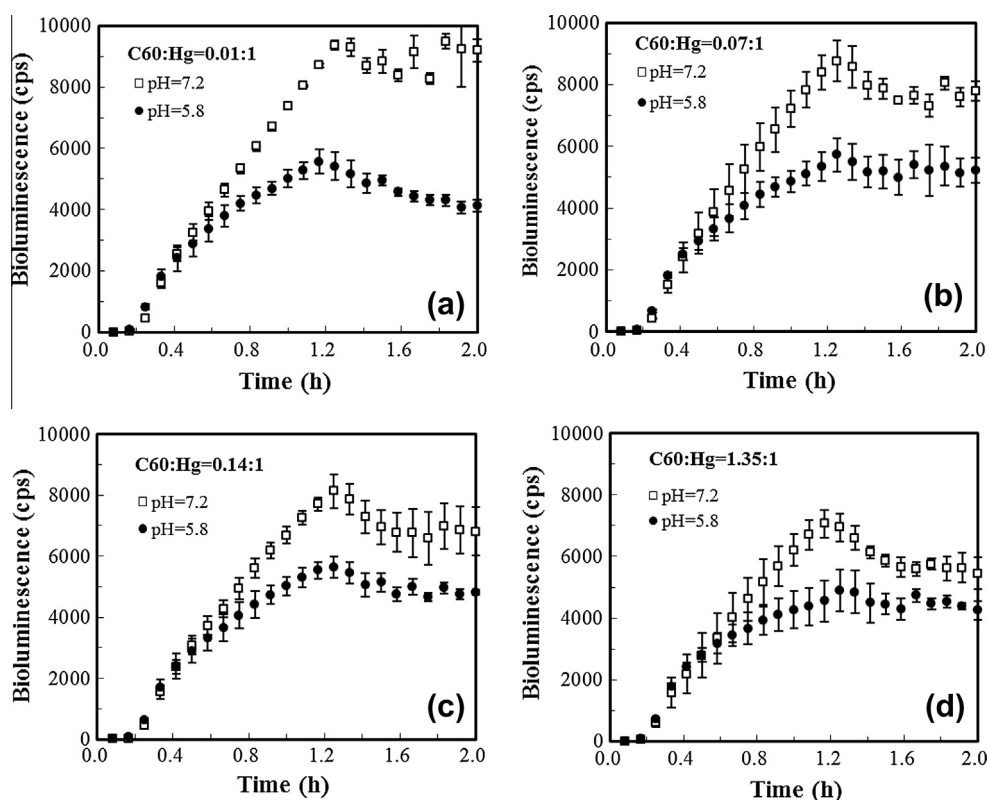


Fig. 4. Effect of pH on mercury bioavailability as measured by the *E. coli* ARL1 bioluminescent bioreporter at C60:Hg mass ratios of (a) 0.01:1, (b) 0.07:1, (c) 0.14:1 and (d) 1.35:1 in the presence of a constant $0.74 \mu\text{g mL}^{-1}$ concentration of Hg^{2+} . cps: bioluminescent counts/s.

- Increases in C60 dosage reduce mercury bioavailability. Thirty percent of Hg^{2+} became unavailable to the ARL1 bioreporter bacteria when the mass ratio of C60 to Hg^{2+} was 0.01.
- The length of reaction time plays a more important role than C60 dosage in reducing Hg^{2+} bioavailability, suggesting slow kinetics of the C60–Hg interactions.
- Lowering the solution pH from 7.2 to 5.8 decreases mercury bioavailability, and this effect is more significant at lower C60 dosages.

Overall, this study provides meaningful insights into the potential of C60 in reducing the biotoxicity of mercury in the environment. The low mass density of C60 makes it easy to disperse in aqueous environments, under appropriate risk assessment controls, especially in wastewater treatment plants and constructed wetlands where water remains relatively stagnant and is susceptible to substantial metal pollution. The large inner surface area of C60 and its strong association with mercury make it a promising candidate for improving existing filtration materials (e.g., activated carbon). Furthermore, the reduction in bioluminescence exhibited by *E. coli* ARL1 in the presence of C60, particularly under acidic conditions, provides insights into the potential of C60 for influencing the overall biotransformation of mercury in the environment. The association of C60 with mercury may also inhibit the cytotoxic effect of C60 on biological cells. Nonetheless, clarification of these issues need further investigation with consideration of natural environmental factors, such as dissolved organic matter and other metal ions.

Acknowledgements

This research was supported by China's Shaanxi Province Key Laboratory of Educational Development (Project No. 11JS076), the Fundamental Research Program of Shaanxi Province Natural Sciences (S2012JC7610), and the University of Tennessee's Center for Environmental Biotechnology and the Institute for a Secure and Sustainable Environment. We would like to thank Daniel Colburn from Oak Ridge High School for his valuable assistance in the experiments.

References

- Colvin, V.L., 2003. The potential environmental impact of engineered nanomaterials. *Nature Biotechnology* 21 (10), 1166–1170.
- Cooper, A.M., Hristovski, K.D., Moeller, T., Westerhoff, P., Sylvester, P., 2010. The effect of carbon type on arsenic and trichloroethylene removal capabilities of iron (hydr)oxide nanoparticle-impregnated granulated activated carbons. *Journal of Hazardous Materials* 183 (1–3), 381–388.
- Dahl, A.L., Sanseverino, J., Gaillard, J.-F., 2011. Bacterial bioreporter detects mercury in the presence of excess EDTA. *Environmental Chemistry* 8 (6), 552–560.
- Golding, G.R., Kelly, C.A., Sparling, R., Loewen, P.C., Rudd, J.W.M., Barkay, T., 2002. Evidence for facilitated uptake of Hg(II) by *Vibrio anguillarum* and *Escherichia coli* under anaerobic and aerobic conditions. *Limnology and Oceanography* 47, 967–975.
- Golding, G.R., Sparling, R., Kelly, C.A., 2008. Effect of pH on intracellular accumulation of trace concentrations of Hg(II) in *Escherichia coli* under anaerobic conditions, as measured using a mer-lux bioreporter. *Applied and Environmental Microbiology* 74 (3), 667–675.
- Jones, A.B., Slotton, D.G., 1996. Mercury effects, sources and control measures, Technical Report of The Regional Monitoring Program, San Francisco Estuary Institute, Richmond, CA.
- Kelly, C.A., Rudd, J.W.M., Holoka, M.H., 2003. Effect of pH on mercury uptake by an aquatic bacterium: implications for Hg cycling. *Environmental Science and Technology* 37, 2941–2946.
- Koh, W., Choi, J.I., Lee, S.G., Lee, W.R., Jang, S.S., 2011. First-principles study of Li adsorption in a carbon nanotube-fullerene hybrid system. *Carbon* 49 (1), 286–293.
- Lesniewska, B.A., Godlewska, I., Godlewska-Zylkiewicz, B., 2005. The study of applicability of dithiocarbamate-coated fullerene C-60 for preconcentration of palladium for graphite furnace atomic absorption spectrometric determination in environmental samples. *Spectrochimica Acta Part B-Atomic Spectroscopy* 60 (3), 377–384.
- Masciangioli, T., Zhang, W.X., 2003. Environmental technologies at the nanoscale. *Environmental Science and Technology* 37 (5), 102A–108A.
- Meyyappan, M., Srivastava, D., 2000. Carbon nanotube – a big revolution in a technology that thinks very, very, very small. *IEEE Potentials* 19 (3), 16–18.
- Miyako, E., Nagata, H., Hirano, K., Makita, Y., Hirotsu, T., 2008. Photodynamic release of fullerenes from within carbon nanohorn. *Chemical Physics Letters* 456 (4–6), 220–222.
- Nanseu-Njiki, C.P., Tchamango, S.R., Ngom, P.C., Darchen, A., Ngameni, E., 2009. Mercury(II) removal from water by electrocoagulation using aluminium and iron electrodes. *Journal of Hazardous Materials* 168 (2–3), 1430–1436.
- Pyrzyska, K., 2007. Application of carbon sorbents for the concentration and separation of metal ions. *Analytical Sciences* 23 (6), 631–637.
- Reiter, L., Falk, H., Groat, C., Coussens, C.M., 2004. From source water to drinking water: workshop summary. In: Roundtable on Environmental Health Sciences, Research, and Medicine. The National Academies Press, Washington, DC.
- Savage, N., Diallo, M.S., 2005. Nanomaterials and water purification: opportunities and challenges. *Journal of Nanoparticle Research* 7 (4–5), 331–342.
- Schindler, D.W., Hesslein, R.H., Wagemann, R., 1980. Effects of acidification on mobilization of heavy-metals and radionuclides from the sediments of a freshwater lake. *Canadian Journal of Fisheries and Aquatic Sciences* 37 (3), 373–377.
- Tawabini, B., Al-Khalidi, S., Atieh, M., Khaled, M., 2010. Removal of mercury from water by multi-walled carbon nanotubes. *Water Science and Technology* 61 (3), 591–598.
- United States Environmental Protection Agency, 1997. Office of Research and Development. Capsule report, aqueous mercury treatment. Report EPA-625-R-97-004, Washington, DC.
- USEPA (United States Environmental Protection Agency), 2009. National Primary Drinking Water Regulations. EPA-816-F-09-004, Washington, DC. <<http://www.epa.gov/ogwdw000/consumer/pdf/mcl.pdf>>.
- Yoon, M., Yang, S., Hicke, C., Wang, E., Geohagan, D., Zhang, Z., 2008. Calcium as the superior coating metal in functionalization of carbon fullerenes for high-capacity hydrogen storage. *Physical Review Letters* 100 (20), e206806.